American Journal of Civil Engineering
2022; 10(1): 1-12
http://www.sciencepublishinggroup.com/j/ajce
doi: 10.11648/j.ajce.20221001.11
ISSN: 2330-8729 (Print); ISSN: 2330-8737 (Online)

Evaluating Wind Erosion Sensitivity for Landfill Sites in New Mexico Using Fuzzy Analytical Hierarchy Process (FAHP)

Clinton Richardson[1, *], Tracy Sadler[2]

[1]Department of Civil and Environmental Engineering, New Mexico Tech, Socorro, New Mexico

[2]New Mexico Environment Department, Air Quality Bureau, Santa Fe, New Mexico

Email address:

clinton.richardson@nmt.edu (C. Richardson), tracy.sadler@state.nm.us (T. Sadler)

[*]Corresponding author

To cite this article:

Clinton Richardson, Tracy Sadler. Evaluating Wind Erosion Sensitivity for Landfill Sites in New Mexico Using Fuzzy Analytical Hierarchy Process (FAHP). *American Journal of Civil Engineering.* Vol. 10, No. 1, 2022, pp. 1-12. doi: 10.11648/j.ajce.20221001.11

Received: December 17, 2021; **Accepted**: January 4, 2022; **Published**: January 15, 2022

Abstract: The final closure veneer for municipal solid waste landfills must be designed to withstand an allowable annual soil loss from wind erosion over its design life. Veneer sensitivity to wind erosion depends on a multiplicity of intertwined variables. A Fuzzy Analytical Hierarchy Process (FAHP) is used to evaluate weightings for specific forcing function criteria to assess overall wind erosion sensitivity (WES) at current and former landfill locations based on input from multiple decision makers selected from consulting, regulatory, and academe sources. FAHP weights represent the degree of importance of a given criteria relative to an overall criterion. For WES assessment, three criteria were identified: climatic factor (CF) as a function of wind power density (WPD) and effective precipitation index (EPI), vegetation cover (VC), and soil erodibility given as a wind erodibility index (WEI). The results revealed almost equal importance for WPD and VC with WEI being the lesser important criteria. Rankings of thirteen landfill locations in New Mexico showed that Las Cruces was most susceptible to wind erosion with Los Alamos and Clines Corner being least susceptible. The assessment methodology is useful for identifying potential hot spots for wind erosion with respect to the design and maintenance of final cover for landfills.

Keywords: Municipal Landfills, Wind Erosion, Fuzzy Analytical Hierarchy Process

1. Introduction

An important challenge in landfill design relates to the final veneer, intended to maximize runoff, enhance evapotranspiration, and minimize vertical percolation into the buried waste. The overall hydrologic water balance at the landfill surface depends on several factors, one of which is the transpiration component, modified by proper selection and management of plant species. Establishing vegetative cover is especially crucial for landfills in arid and semi-arid regions, such as New Mexico. A sparse or absent ground cover does little to effect removal of any stored water from the veneer between precipitation events; in addition, the surface is susceptible to soil loss from wind erosion, further exacerbating establishment of a viable vegetative cover. In addition, aeolian transport is a major cause for loss of soil nutrients in susceptible environments and a key abiotic factor influencing overall ecosystem dynamics [1, 2].

Soil erosion by wind is a continuous and dynamic natural geomorphological process having major impact on arid and semi-arid lands. The magnitude and rate of soil movement depends upon a number of intertwined factors. Climate (wind intensity and patterns, frequency and amount of precipitation), soil properties (texture, moisture, structure, organic matter content), site topography (exposure, elevation, surface roughness), and vegetation (type, amount, status), all influence the extent and severity of wind erosion. A generalized overview of key variables is provided in Section 2.

New Mexico Solid Waste Management Regulations NMAC 20.9.6 A (1) (c) stipulate a closure veneer for minimizing erosion to consist of a minimum of six inches of earthen material capable of sustaining native plant growth. The Application for Permit for new landfills must provide evidence through engineering calculations that the estimated

soil erosion through water and wind transport does not exceed an allowable loss of 5 tons/ac/yr (11.2 mt/ha/yr) each for the proposed final veneer design. Wind erosion calculations are typically estimated using the Wind Erosion Prediction System (WEPS) model [3].

In this research key wind erosion criteria were selected to evaluate soil wind erosion hazard for selected landfill locations in New Mexico using a fuzzy analytical hierarchy process (FAHP) pair-wise comparison to weight each criteria. Traditional AHP is a Multi-Criteria Decision Making (MCDM) linguistic model to address decision making problems affected by several conflicting factors. AHP lacks the ability to deal with vagueness and uncertainty in subjective personal judgement through its single crisp value pair-wise comparisons; however, FAHP allows the decision maker to express approximate or flexible preference using triangular fuzzy numbers (TFNs) and linguistic variables to achieve a higher level of accuracy and consistency of judgement [4]. Additionally, multiple experts may be integrated within both AHP and FAHP to yield a synergistic aggregation of individual judgements based on a geometric mean of pair-wise comparison responses [5].

2. Wind Erosion Variables

Table 1 provides an overview of the various wind and soil parameters that are controlling wind erosivity and soil erodibility during a wind erosion event.

Table 1. *General parameters that influence wind erosivity and soil erodibility.*

Wind Erosivity	**Soil Erodibility**	
	Soil and Aggregate Parameters	**Surface Parameters**
Wind Direction	Grain Size and Erodible Fraction	Vegetation (Height, Orientation, & Density)
Velocity	Aggregate Height	Soil Moisture
Frequency	Dry Soil Stability	Soil Roughness
Duration	Aggregate Orientation	Surface Length
Area	Organic Content	Topography
Turbulence	Clay Content	Field Length
Shear Stress	Calcium Carbonate Content	Surface Crust

2.1. Soil Erodibility

Soil erodibility is controlled by intrinsic physical and chemical properties of soils. Soil texture and structure affect wind erosion risk. Texture is an indication of the relative content of particles of various sizes, specifically percent sand, silt, and clay, and classified using a USDA soil textural triangle. Structure is the combination of individual soil particles into aggregates. Erodibility as originally evaluated by Woodruff and Siddoway [6] is the potential soil loss in mass per unit area per year (tons/ac/yr or mt/ha/yr) from a wide, unsheltered, isolated field with a bare, smooth, non-crusted surface. Soils with an erodible fraction greater than 60% are generally considered at high erosion risk [7].

Sandy textured soils are highly susceptible to wind erosion; whereas clayey textured soils have low erodibility; however, clayey textured soils broken up by repeated freeze and thaw cycles are also erodible. Such cycles induce increases in porosity that lead to weakened cohesive forces within the soil structure, which contributes to increases of the soil erodible fraction [8]. Soils would be more susceptible to wind erosion during the late winter, early spring period for arid and semi-arid regions following significant freeze-thaw cycles. Development of a biological soil crust by a consortium of soil microbes contributes to soil stability, especially in arid and semi-arid landscape, by binding soil particles together [9]. Using a portable wind tunnel, threshold velocities observed for soil movement for highly erodible soils at the Jornada Experimental Range in south central New Mexico were well above wind velocities. Induced disturbances by foot or vehicular traffic resulted in threshold velocities well below regional wind velocities.

Multiple regression equations have been developed to estimate soil erodibility based on percentage of sand, silt, clay, organic matter, and $CaCO_3$ content [10, 11]. A Wind Erodibility Index (WEI) in units of tons/ac/yr is also available through the USDA Web Soil Survey geographic database [12] by isolating an area of interest within the contiguous US, Hawaii, Alaska, and other selected regions using latitude and longitude coordinates. Table 2 provides a general overview of soil erodibility for selected soil textures [13].

Table 2. *Erodibility Index for Soil Texture Classes [13].*

Soil Texture	**Erodibility Index (mt/ha/yr)**
Sand	494
Sandy Loam	409
Loam	308
Clay	246
Clay Loam	196

2.2. Soil Moisture

Soil erodibility or its resistance to wind erosion intrinsically depends upon moisture content or lack thereof. Soil entrainment by wind varies approximately inversely as the square of effective surface soil moisture [14]. Sirjani et al. [15] observed a statistically significant exponential relationship of decreasing areal mass loss rate with soil moisture using a portable wind tunnel conducted at 15 m/s wind speed for 20 different arid and semi-arid regions in Iran. A critical value whereby wind erosion was inhibited was 2% gravimetric moisture content. Inhibited erosion was also reported for clay content greater than 15%.

Using wind tunnel tests Weinan et al. [16] showed that the threshold wind velocity needed to mobilize sandy loam soils

increases with increasing soil moisture, exhibited by a negative exponential function. With increased soil moisture, the wind erosion rate rapidly decreased. A critical moisture content of 4% was reported where the rate became essentially constant.

Detailed surface soil moisture is generally not available for different geographic locations; however, effective soil moisture may be assumed proportional to an aridity index. These surrogates indicate the magnitude of water deficit in the top surface layer. When this layer has lost sufficient moisture content necessary for interparticle bonding, wind entrainment is possible. Aridity or degree of soil dryness is not just a function of precipitation alone. Temperature is a factor as well. One such index is the annual Thornthwaite Effective Precipitation Index (EPI), computed from the monthly values of precipitation (mm) and evaporation, wherein evaporation is expressed in terms of temperature (°F) [17]:

$$EPI = 3.16 \sum_{1}^{12} \left\{ \frac{P}{T-10} \right\}^{10/9} \quad (1)$$

Climate classification based on annual EPI is less than 15 and between 16 and 31 for arid and semi-arid aridity regimes, respectively.

Gamo et al. [18] classified arid lands using a modified Thornthwaite Potential Evaporation Index as an aridity index. For classified semi-arid regions, a vegetation index expressed as a long-term yearly maximum Normalized Difference Vegetation Index ($NDVI_{max}$) was linearly proportional to this modified aridity index.

2.3. Wind Intensity

Soil erosion is eminent when the destabilizing forces of drag and lift exerted by the air stream exceed the stabilizing forces of gravity and interparticle cohesion [19]. There is a critical threshold when soil movement occurs, typically expressed as threshold velocity that depends on a multiplicity of factors, such as surface roughness, shape and size of the soil aggregate, and soil moisture and clay content. Zhou et al. [11] evaluated large-scale wind erosion in Mongolia using the AHP approach. Here, a critical wind field intensity for use in AHP pair-wise comparisons was defined by the number of days where wind speed exceeded 6 m/s.

Soil erosivity or the rate of soil movement is proportional to wind power density (WPD) [20], which varies with the cube of wind velocity and is keyed to a specific threshold velocity. The definition used in the WEPS model [3] is given as:

$$WPD = \frac{1}{2}\rho(u - u_t)u^2 \quad (2)$$

where ρ = air density (kg/m^3); u = wind speed (m/s) at 10 m height; and u_t = threshold wind speed when soil movement starts to move and entrain (m/s). A threshold velocity of 8 m/s is typically considered as a minimum; however, higher values have been used for less erodible soils [21]. The units for WPD are J/m^2/s or m^3/s^3. Monthly values for the US typically range between 10 and 100 m^3/s^3 [22]. In the WEPS model, that uses a threshold velocity of 8 m/s, WPD is given in kJ/m^2/d (10 m^3/s^3 = 1101 kJ/m^2/d). WPD data are available in the WEPS model for selected cities in New Mexico.

2.4. Vegetation Cover

New Mexico land cover is dominated by shrubland (48%) and includes expanses of grasslands (31%) and evergreen forests (17%) [23]. Low perennial cover typical of arid and semi-arid regions, however, leaves the landscape exposed and vulnerable to wind erosion. Thus, vegetative cover plays a dominant role in mitigating wind erosion from an erodible landscape. Soil erosion varies with the total cross-sectional silhouette area of the vegetative material. Removal of soil from beneath or between natural vegetation covers depends on the width, height, density, and distribution of cover types relative to wind direction and strength. Vegetation provides additional surface roughness that influences wind erosion directly by sheltering the surface from erosive winds and by absorbing a portion of the wind momentum flux, reducing the shear stress at the soil surface [24]. Munson et al. [25] reported soil mass flux from four shrubland test plots in southeastern Utah following a 17.5 m/s wind event. For both medium and high intensity soil disturbances of the developed biological soil crust, an exponential decrease in flux was observed with increased perennial vegetative cover.

Meng et al. [26] performed a multi-factorial analysis and model simulation of field wind tunnel data collected in a semi-arid region of northern China, based on vegetation coverage, wind speed, and soil moisture. Vegetation coverage was found to be a dominant factor controlling wind erosion by lowering the threshold velocity and increasing surface roughness. A critical level of coverage was found to be 60% for effective control of wind erosion. Based on model simulation of the interactive effects of the three criteria, mass flux of eroded sand was in the following order: wind speed, vegetation, and soil moisture. Yan et al. [27] evaluated six levels of vegetation coverage (0% to 95%) for an experimental field study, using uniform clusters of plants arranged in the dominant wind direction. Minimum threshold velocity to initiate soil loss was 6.2 m/s. Soil loss was determined as a function of vegetative cover for different periods of study. A critical vegetative coverage to minimize impact on soil texture and soil nutrients was judged to be greater than 35%.

Many natural range landscapes in the southwest US have less than 35% foliar cover [28]. Weltz et al. [29] measured canopy and ground surface cover for Chihuahuan Desert shrubland and Chihuahuan Desert grassland in Arizona. Canopy and ground surface cover were 32.2% and 82.7%, and 30.5% and 39.3%, respectively, for the two land covers. Ground surface cover included bare soil, rocks, litter, and basal plant cover. In addition, shortgrass prairie land cover near Cuba, New Mexico had 30.5% canopy cover and 61.7% ground surface cover.

Information on actual levels of vegetation coverage for landfills in arid and semi-arid regions is limited. Anderson

and Stormont [30] stated that in many such landfills natural vegetation will cover only 10 to 20% of the surface veneer. Breshers et al. [31] evaluated two different landfill cover designs for water balance and vegetation cover more than a decade after installation at Los Alamos National Laboratory in Los Alamos, New Mexico. Ground cover was high ranging from 69% to 100% coverage for the four test plots; however, species diversity differed between the two designs in terms of magnitude and relative proportion of original vegetation and invasive species. As part of a five-year field demonstration project in Albuquerque, New Mexico on alternative landfill covers conducted by Sandia National Laboratories, vegetation cover was assessed in terms of plant type (grass, weed, forbs, and shrubs), density, and cover [32]. Total vegetation cover varied annually and seasonally with each landfill cover design and reflected the precipitation received over the period of study (wet versus dry). The evapotranspiration (ET) cover improved the most over the five years, with vegetation cover reported at 12.7%, 62.3%, and 16.8%, respectively, for Fall 1998, Fall 1999, and Fall 2000.

In arid and semi-arid regions, satellite imagery has been used to estimate vegetation cover using spectral measurements [11, 13, 33-37]. One of the most used and implemented indices calculated from multispectral information as a normalized ratio between the red and near infrared bands is the Normalized Difference Vegetation Index (NDVI) first proposed in 1974 [38]. With green vegetation cover visible red light is strongly absorbed, while near infrared light is strongly reflected:

$$NDVI = \frac{(NIR-R)}{(NIR+R)} \quad (3)$$

where R and NIR stand for the spectral reflectance measurements acquired in the red (visible) and near-infrared regions, respectively. NDVI values range from -1 to +1 with vegetated areas ranging from 0.4 to 1. In GIS applications, a single-band 8-bit raster is used to scale the maximum and minimum NDVI values to a 0 to 255 range. Adjustments have been applied to satellite imagery for sparse vegetation in arid and semi-arid environments to accommodate variability due to high soil background [37].

In the semi-arid region of central New Mexico, Weiss et al. [33] observed a pre-monsoon NDVI minimum in late spring and early summer and a bimodal NDVI having a late-early summer initial peak, a mid-to-late summer pre-monsoonal dip, and a second maximum peak in early autumn that paralleled the bimodal precipitation pattern. The authors noted, however, that vegetation canopies in arid and semi-arid environments do not achieve complete coverage, lending uncertainty to NDVI as to the spectral influence of soil and soil moisture between gaps in the cover. Eleven-year average spring and summer NDVI ranged between 108 and 127 and between 109 and 131, respectively, for six vegetation communities examined, based on a scale 0 to 200. Bulut et al. [39] produced an annual average maximum NDVI map for New Mexico that ranged from 115 to 160 for years 1995-2009 based on a scale of 0 to 255.

Hagen et al. [40] developed a soil adjusted total vegetation index (SATVI) to map total vegetation cover for the western US rangelands using MODIS data scaled and calibrated with ground truth measurements. Included in the ground truth campaign was six sites in Arizona and New Mexico. For low values of SATVI, the 90% prediction limit for cover was ± 10%. An eight day MODIS SATVI colored coded map of long-term average (2000-2010) total vegetation cover indicated that the majority of New Mexico was below 50% coverage.

2.5. Wind Fetch Length and Site Orientation

Soil erosion depends on total distance across a given landscape measured along the dominant wind erosion direction [41]. The physical unsheltered field length impacted by the dominant wind depends on the actual field dimensions, field orientation, and wind direction [42].

An unsheltered landscape with its broad side at right angles to and its narrow side parallel with the prevailing wind direction will have minimum overall rate of erosion [42]. Using frequency of winds for specific cardinal directions (Wind Rose), for example N, S, E, W, NE, SW, SE, and NW, a weighted mean unsheltered field length may be estimated as well [44].

On an unsheltered planar landscape, mass flux is zero on the windward edge and increases with distance to leeward side until the air stream becomes saturated and transport capacity is maximum. The distance required to reach this maximum on a given soil is the same for any erosive winds [6]; however, at some point the rate of increase in mass transported becomes limited by the erosion rate at the soil surface [45]. A critical fetch length exists. Erosion rates are greater for highly erodible soils; thus, the length required to reach maximum capacity is shorter. Beyond this critical length, the rate of increase in transported mass gradually decreases and approaches zero at air stream saturation. Fryrear and Saleh [45] evaluated field test results fitted to a sigmoid curve to examine the relationship between fetch length and maximum transport capacity and to estimate a critical fetch length specified at 63% of maximum transport capacity. Depending on wind and field conditions for the test sites, critical fetch length varied from 31 to 129 m. However, critical fetch lengths of more than 300 m have been reported based on analysis of field data [46].

2.6. Land Surface Slope Gradient and Relief

Early wind tunnel and field studies on wind erosion were conducted on flat or relatively flat soil surfaces. A study was conducted by Zhang et al. [47] for a bare silty loam soil under natural meteorological conditions on the Chinese Loess Plateau using six slope gradients (0°, 5°, 10°, 15°, 20°, and 25°) showed that wind erosion rates increased with increasing slope gradients. A two-year average increasing rate was much lower from 20° to 25° compared to lower slope gradients, indicating that 20° was a turning slope

gradient for the variation of erosion by wind, and that the critical erosion gradient was not lower than 25°. Typical landfills are designed at 4H:1V (14°) outside vegetative slope.

Shi et al. [34] included land surface relief as a factor to assess large-scale spatial wind erosion hazard on the Mongolian Plateau using ArcGIS processing of the digital elevation model (DEM) to obtain an average degree of land relief. Six classes of wind erosion hazard was specified based on the distribution of four factors: vegetation coverage, soil dryness, wind energy intensity, and land surface relief.

3. New Mexico Climate

New Mexico has a mild, arid or semiarid, continental climate characterized by light precipitation totals, low relative humidity, and a relatively large annual and diurnal temperature range [48].

3.1. Precipitation

Average annual precipitation ranges from less than 10 in (254 mm) over much of the southern desert and the Rio Grande and San Juan Valleys to more than 20 in (508 mm) at higher elevations, with wide variation in annual totals throughout the state typical of arid and semiarid climates. Seasonal precipitation is distinctly bimodal with less-intense spring rains and late summer monsoonal rains. Precipitation occurs primarily from May through October, comprising 60% to 80% of the total yearly precipitation in the northwestern plateau and eastern plains of the state, respectively.

3.2. Relative Humidity

Relative humidity ranges from an average of near 65% about sunrise to near 30% in midafternoon; however, afternoon humidity in warmer months is often less than 20% and may go as low as 4%. In arid regions changes in surface soil moisture associated with variations of air humidity significantly affect soil susceptibility to wind erosion [49].

3.3. Temperature

During summer months, individual daytime temperatures quite often exceed 100° F (38°C) at elevations below 5,000 ft (1524 m). Average monthly maximum temperatures during July range from slightly above 90° F (32°C) at the lower elevations to the upper 70's°F (20's°C) at higher elevations. The freeze-free season ranges from more than 200 days in the southern valleys to less than 80 days in the northern mountains. Minimum temperatures below freezing are common through the state during winter, potentially subjecting surface soils to periodic freeze-thaw cycles.

3.4. Evaporation

Potential evaporation in New Mexico is much greater than average annual precipitation. During the warmest months May through October, evaporation from a Class A pan ranges from near 41 in (1041 mm) in the north-central mountains to 73 in (1854 mm) in the southeastern valleys.

3.5. Wind Speed and Direction

Wind speeds are usually moderate, although relatively strong winds often accompany occasional frontal activity during late winter and spring months. Frontal winds may exceed 30 mph (13.4 m/s) for several hours and reach peak speeds of more than 50 mph (22.4 m/s). Spring is the windy season in New Mexico. Winds are generally stronger in the eastern plains. Winds generally predominate from the southeast in summer and from the west in winter. Local surface wind directions vary greatly due to local topography and mountain and valley breezes.

4. Selection of FAHP Wind Erosion Factors

Three basic criteria were initially selected to evaluate wind erosion potential for landfills using the FAHP approach for thirteen cities and towns within New Mexico: climatic factor, soil erodibility, and vegetation cover. Slope gradient was not considered although landfills are designed for a relatively flat top veneer (2° to 5°) with a typical side slope of 4H:1V (14°). In addition, site-specific wind rose data is limited for many landfill sites in New Mexico in order to establish the dominant wind direction. Therefore, estimating a site-specific unsheltered wind length (WL) is not possible with Eq. 4. The assumption used herein is that most landfill dimensions are sufficiently large in length and width and landfill orientation is such that the unsheltered wind length across the closure veneer would most likely exceed the critical wind fetch length.

4.1. Climatic Factor

Lyles [50] developed climatic factors (CF) for the west based on earlier work by Chepil et al. [51], wherein CF was a function of average monthly wind speed (m/s) and Thornthwaite Effective Precipitation Index (EPI):

$$CF = 386\frac{u^3}{EPI^2} \quad (4)$$

where u = average monthly wind speed and EPI as previously described.

However, WPD is available through the WEPS model as monthly averages and as an annual average expressed as kJ/m^2/d. For the present analysis, CF is re-defined as:

$$CF = \frac{WPD}{EPI^2} \quad (5)$$

EPI was calculated based on long-term average monthly averages for temperature and precipitation for New Mexico [52]. As WPD increases and EPI decreases for a given location, the sensitivity to wind erosion increases as EPI may be interpreted as an indirect measure of soil dryness. Figure 1 provides an annual plot of monthly WPD (8 m/s threshold velocity) and EPI data for Albuquerque. Figure 2 shows the

calculated monthly CF for selected locations. The period from January to June shows high WPD and low EPI with a peaked CF. Similar patterns were noted for the thirteen locations data set.

4.2. Soil Erodibility

An area-weighted Wind Erodibility Index (WEI) expressed as soil loss in units of ton/ac/yr converted to mt/ha/yr was obtained for applicable landfill latitude and longitude coordinates using the USDA Web Soil Survey [12].

4.3. Vegetative Cover

Vegetation plans for closure of landfills in New Mexico typically specify a drought tolerant native species seed mix, seed application rate, and watering rate to promote initiation of adequate cover for erosion control. However, a long-term well-developed cover is seldom achieved, with actual coverage varying considerably throughout the state. To evaluate critical coverage during the windy season, a long term average NDVI was calculated for March through June from 2013 to 2019.

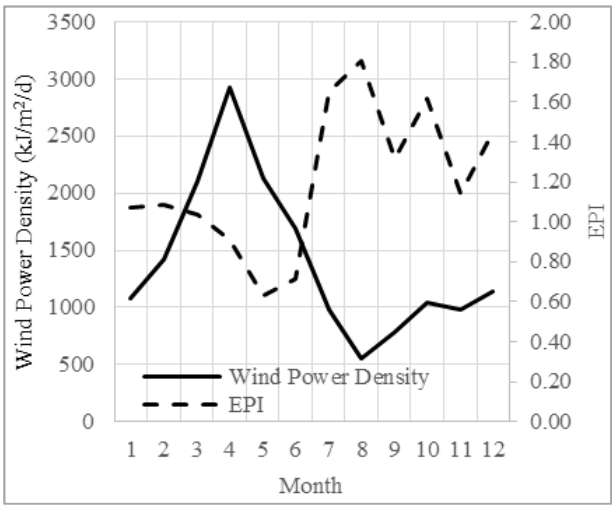

Figure 1. *WPD and EPI for Albuquerque, New Mexico.*

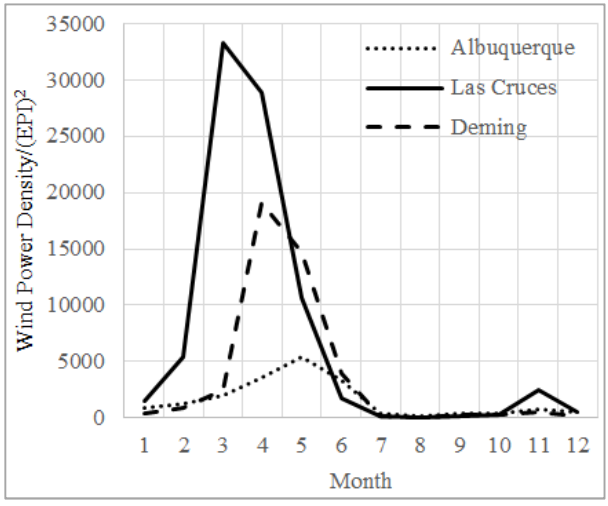

Figure 2. *Climate Factor (CF) for Selected Cities in New Mexico.*

5. Fuzzy Analytical Hierarchy Process (FAHP) Methodology

5.1. Triangular Fuzzy Number (TFN) Membership Functions

The fuzzy AHP used for weighting of wind erosion criteria applies the triangular fuzzy number (TFN) through a triangular membership function (μ_A) from 0 to 1 defined by three real numbers, expressed as a lower value, mean value, and an upper value (l, m, and u), where

$$\mu_A(x) = \begin{Bmatrix} 0, x < l \\ \left\{\frac{(x-l)}{(m-l)}\right\}, l \le x \le m \\ \left\{\frac{(u-x)}{(u-m)}\right\}, m \le x \le u \\ 0, x > u \end{Bmatrix} \quad (6)$$

5.2. Fuzzy Pair-Wise Comparison Matrix (FPCM)

A crisp pair-wise comparison matrix (PCM) based on a linguistic interpretative scale ranging from 1 to 9 [53] is fuzzified using a triangular fuzzy number for each scale value. One such correlation between the numerical value of TFNs and the linguistic variables is given in Table 3, where the reciprocal of the TFN, M_i^{-1}, is denoted as ($1/u_i$. $1/m_i$, and $1/l_i$). Intermediate TFNs can be incorporated in the FAHP as well. The lower and upper bounds represent an uncertainty and vagueness range within the judgement expressed by the decision maker.

Table 3. *Scale of Relative Importance Used for Pair-wise Comparison Matrix.*

Intensity of Importance and Resultant Fuzzy Number*	Judgement	TFN
1→1*	Equally Important	(1,1,1)
3→3*	Weakly Important	(2,3,4)
5→5*	Fairly Important	(4,5,6)
7→7*	Strongly Important	(6,7,8)
9→9*	Absolutely Important	(8,9,10)

Table 4 is an example of an initial comparison matrix for a set of three basic criteria. The numbers on the top row of Table 3 relate to the intensity of importance for one criteria over another criteria with fuzzy preference intervals denoted in Table 2. Each expert populates a Table 3 separately. Only one check mark per row is allowed for C1 versus C2; C1 versus C3; and C2 versus C3 comparisons. For example, one expert might rank C1 as being *Fairly Important* (5) than C2 and C3 being *Weakly Important* than C1 (3) and C2 being *Equally Important* as C3 (1). Table 3 is then re-populated with all intensities of importance data from participating experts with each row having n populated values equal to the number of experts. This yields a composite initial matrix that will be transformed into an integrated fuzzified pair-wise comparison matrix using a geometric mean of fuzzy triangular functions from individual pair-wise responses [5].

Table 4. *Initial Comparison Matrix.*

	Left Criteria Greater					Right Criteria Greater				
	9	7	5	3	1	3	5	7	9	
C1			X							C2
C1						X				C3
C2					X					C3

5.3. Consistency Check

Subsequent manipulations of the integrated matrix yields a final check for consistency. The principle idea of FAHP judgements relies on the consistency of the fuzzy pair-wise comparison matrix (FPCM). The more consistent a FPCM is, the closer the computed maximum eigenvalue (λ_{max}) is to the number of criteria. To ensure that the FAHP judgements are reliable and sufficiently accurate, a consistency ratio (CR) is determined [53]:

$$CR = \left\{ \frac{\frac{(\lambda_{max} - n)}{n-1}}{RI} \right\} \quad (7)$$

where λ_{max} = maximum eigenvalue of the FPCM; n = number of criteria elements being compared; and RI = a random consistency index based on the number of criteria. The FPCM is acceptable if CR is less than 0.10 [53]. If CR exceeds 0.10, then the linguistic interpretation of intensity of importance for the selected criteria needs reconsideration. The process is repeated until an acceptable threshold is achieved. If consistent, the respective weighting factors for each criterion are then determined.

5.4. Defuzzification of Fuzzy Pair-Wise Comparison Matrix

Determining the crisp weight of each criteria from the integrated fuzzy comparison matrix uses the fuzzy extent analysis (FEA) method by Chang [54] with the Wang et al. [55] modification of the normalization process applied to calculate the values in the fuzzy synthetic extent *n* x *n* matrix (FSEM). Methods for defuzzification of the synthetic extent matrix to generate criteria weights include the centroid and the alpha cut/lambda function methods.

The centroid method calculates the average for row *i* in the FSEM as (l_i+ m_i +u_i)/3, which are summed to give a total for *n* rows. Respective crisp criteria weights (w_i) are determined by dividing row *i* centroid average by the total. The alpha cut/lambda method [56] accounts for uncertainty and optimism in the FAHP. Herein the method is applied to the synthetic extent matrix to generate crisp criteria weights. Alpha (α) takes on values from 0 to 1, for most uncertainty to least uncertainty. Lambda (λ) represents the attitude of the decision maker from 0 to 1, for pessimistic to optimistic.

$$\alpha_{left} = \{\alpha(m - l) + l\} \quad (8)$$

$$\alpha_{right} = \{r - [\alpha(r - m)]\} \quad (9)$$

where *l, m, r* = left, middle, and right values of a row *i* in the FSEM and where each row represents a given criteria. The crisp value ($C_{i,\lambda}$) for a given criteria is then determined as:

$$C_{i,\lambda} = \lambda * \alpha_{right} + \{(1 - \lambda) * \alpha_{left}\} for\ row\ i \quad (10)$$

Finally, the crisp values are normalized to yield the crisp criteria weights (w_i):

$$w_i = \frac{C_{i,\lambda}}{\sum_1^n C_{i,\lambda}} \quad (11)$$

6. Results

For each of the wind erosion criteria (CF, WEI, and VC) input values were normalized from 0 to 1 for the data set to allow a calculation of a FAHP wind erosion metric (0 to 1) for each location based on derived criteria weights.

6.1. Wind Power Density

For the spring windy period in New Mexico, Las Cruces had the highest maximum monthly WPD at 7463 kJ/m^2/d, with Los Alamos having the lowest maximum monthly WPD at 656 kJ/m^2/d. The highest March to June average monthly WPD was 5400 kJ/m^2/d for Las Vegas, with Los Alamos having the lowest average monthly WPD at 486 kJ/m^2/d. Table 5 shows the simulated WEPS WPD data for the selected locations.

6.2. Effective Precipitation Index

The EPI_{12} ranged from 13.2 for Las Cruces to 39.6 for Los Alamos, indicating a statewide arid and semi-arid climate. A January to June single month EPI_1 taken as a measure of soil dryness varied from a low of 1.08 for Albuquerque to a high of 4.21 for Los Alamos. A May to June total EPI_4 varied from 1.79 for Las Cruces to 10.34 for Los Alamos (Table 4), denoting a drier versus less dry local climate, respectively. Overall, these EPI_4 estimates indicate a relatively low degree of soil dryness over the windy period.

6.3. Climate Factor

The critical period CF was evaluated using Eq. 6. The maximum CF for January to June was 33247 for Las Cruces and 140 for Los Alamos. The January to June average CF was 13597 for Las Cruces and 71 for Los Alamos. All locations exhibited a peak CF between January to June similar to Figure 2.

6.4. Wind Erodibility Index

Table 5 shows values of WEI (mt/ha/yr) taken from USDA Web Soil Survey at specific landfill location coordinates. This soil erodibility represents an area-weighted average of the soil units at each site. Hobbs had the highest WEI with Las Vegas the lowest WEI.

6.5. Vegetation Cover

Figure 3 shows the relationship between vegetative cover expressed as NDVI (Eq. 3) and EPI_{12} (Eq. 1). Although significant scatter is evident, an upward trend in vegetative cover is noted as the aridity index increased similar to that

indicated by Gamo et al. [18]. Percent vegetative cover was also estimated based on a linear relationship with EPI_{12}, scaled between poor cover (20%) and good cover (70%) (not shown). This assumed range draws upon values reported in the cited literature for arid and semi-arid rangelands [28-32, 40]. Based on this approach, vegetative cover ranged from 23% at Las Cruces to 69% at Los Alamos.

6.6. Final FAHP Rankings

Table 6 shows the integrated PCM for six experts using the template from Table 4. Experts included two landfill design consultants, two New Mexico Environmental Department Solid Waste Bureau landfill inspectors, one soil scientist, and one environmental engineering academician. The calculated maximum eigenvalue (λ_{max}) was 3.04, with a consistency ratio (CR) of 0.03, which is less than 0.10. The integrated PCM is, therefore, consistent.

Table 7 provides the fuzzy synthetic extent matrix with the Wang et al. [55] modified normalization applied for determining the extents.

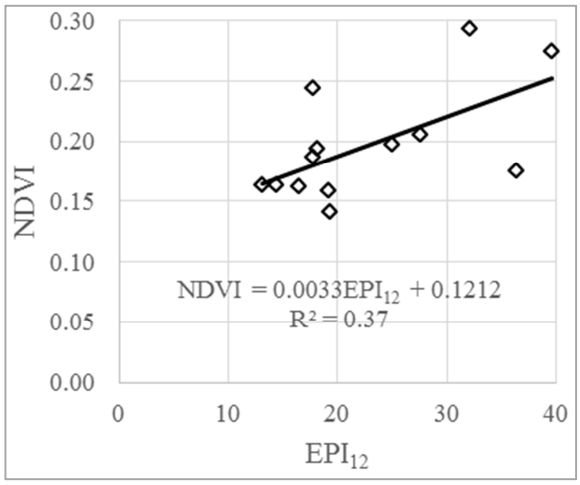

Figure 3. *NDVI versus EPI_{12} for Landfill Sites.*

Using the centroid defuzzification method and subsequent normalization, the criteria weights are CF (0.420), WEI (0.185), and VC (0.395). The alpha cut/lambda function method ($\alpha = 0.5$ and $\lambda = 0.5$) and subsequent normalization gave criteria weights of CF (0.419), WEI (0.190), and VC (0.391). Both defuzzifications are virtually identical.

Based on applying the above criteria weights, a FAHP wind erosion metric was calculated as shown in Table 5, along with the final ranking as to wind erosion sensitivity.

7. Discussion

7.1. Vegetation Cover

Given the weight assigned to vegetative cover, wind erosion sensitivity heavily depends upon an accurate assessment of this major resistive force to soil loss. Torno et al. [58] modeled dust emissions from a landfill surface in northern Spain using computational fluid dynamics (CFD). Average wind velocity measurement taken along the landfill length tracked CFD simulations ($r^2 = 0.93$). Field monitoring of maximum and minimum emissions ($kg/m^2/yr$) from three land treatments (bare, short grass, and tall grass and bushes) from 12 erosion wind events paralleled CFD predictions. The latter land treatment had the lowest emissions with the former being the highest emissions. Thus, assessing wind erosion sensitivity for a given landfill location depends on an accurate measurement of vegetative cover.

Projections of potential landfill vegetative cover based on an effective precipitation index (EPI) and arbitrary, yet reasonable, percent maximum and minimum cover estimates gleaned from the literature for arid and semi-arid lands does not lend itself to a high degree of confidence in a wind erosion sensitivity analysis. However, NDVI estimates produced from satellite imagery have been used as a surrogate vegetation cover in large-scale wind erosion sensitivity studies [11, 59, 60]. Hagen et al. [40] scaled and calibrated satellite imagery with ground truth measurements to develop a regional soil adjusted index of cover. However, the cover accuracy needed at the local scale requires ground-based methods.

7.2. Soil Erodibility

Even though soil erodibility has the lowest weighting, to facilitate a more robust assessment of wind erosion sensitivity, soil erodibility should be calculated based on laboratory analysis of the erodible topsoil for percent sand, silt, clay, organic carbon content, and calcium carbonate content, and an empirical relationship such as used by Zhou et al. [11]. The WEI used herein is part of the USDA Web Soil Survey SSURGO database. Although developed from field observations and laboratory analyses and grounded on science-based interpretations of soil characteristics, WEIs so derived may not be detailed enough to provide the level of accuracy needed at the site-specific level. To validate these interpretations and confirm the identity and characteristics of on-site soils, an in-depth investigation would be needed. Additionally, inventories of wind-blown soil loss collected from field monitoring would allow for better assessment soil erodibility; however, this too requires an investment of human resources and equipment.

7.3. Criteria Weighting

The results herein show that climatic factor (CF) and vegetation cover (VC) were relatively equal in importance for wind erosion sensitivity with much less importance associated with the soil erodibility (WEI). Using the crisp AHP degree of importance scale (1 to 9) for soil erodibility (based on soil texture and organic carbon content), aridity index (Eq. 1), days with wind intensity greater than 6 m/s, and vegetative index (NDVI) assigned by Zhou et al. [11] and applying the FAHP method described herein reveals a weight ordering of vegetative index (0.403), wind intensity (0.359), aridity index (0.171), and soil erodibility (0.069). A similar FAHP exercise for the same four criteria with crisp

AHP degree of importance scale (1 to 9) assigned by Guo et al. [60] gave a weight ordering of vegetative index (0.462), wind intensity (0.285), soil erodibility (0.178). and aridity index (0.075) These orderings of importance are similar with respect to soil erodibility being less important than measures of vegetative cover and wind velocity, with mixed results for aridity (soil dryness), the latter being a function of precipitation and temperature.

Table 5. *Summary of Input Data and FAHP Results.*

Location	Wind Power[1] ($kJ/m^2/d$)	Effective Precipitation Index[2] (EPI_4)	Wind Erodibility Index[3] (WEI) mt/ha/yr	Vegetative Cover[4] (NDVI)	FAHP Wind Erosion Metric[5]	Wind Erosion Sensitivity Rank
Alamogordo	1044	2.92	301	0.159	0.202	6
Albuquerque	2212	3.29	278	0.164	0.216	5
Carlsbad	2951	4.75	560	0.194	0.356	2
Clines Corner	601	8.61	159	0.175	0.086	13
Clovis	4168	8.94	166	0.206	0.125	10
Deming	3016	2.72	237	0.141	0.320	3
Farmington	1540	3.96	194	0.162	0.144	9
Hobbs	1925	7.67	560	0.197	0.282	4
Las Cruces	2536	1.79	239	0.164	0.534	1
Las Vegas	5400	10.34	122	0.294	0.139	8
Los Alamos	486	10.15	125	0.275	0.109	12
Roswell	1513	5.17	179	0.187	0.125	10
Tucumcari	3650	5.17	160	0.244	0.182	7
	Maximum					
	4844	10.34	560	0.294	0.534	
	Minimum					
	488	1.79	122	0.141	0.086	

[1] Average based on March through June data taken from NRCS WEPS for New Mexico [57].
[2] Based on March through June data taken from US Climate Data for New Mexico [52].
[3] Weighted areal average wind erodibility index taken from USDA Web Soil Survey [12].
[4] NDVI averaged data from 2013 to 2019 for March through June using an area of interest having a 1 km radius with respect to each landfill latitude and longitude coordinates.
[5] Fuzzy Analytical Hierarchy Process weighting factors: Climate Factor (0.419); WEI (0.190); and Vegetative Cover (0.391) using normalized input values scaled from 0 to 1.

Table 6. *Integrated Fuzzy Pair-wise Comparison Matrix.*

	CF			WEI			VC		
CF	1	1	1	1.7411	2.1867	2.5508	0.5610	0.8635	1.1761
WEI	0.3920	0.4573	0.5743	1	1	1	0.4353	0.6826	1.0238
VC	0.8503	1.1581	1.7826	0.9767	1.4651	2.2974	1	1	1

Table 7. *Fuzzy Synthetic Extent Matrix.*

Fuzzy Weights (w_i)			
CF	0.2662	0.4127	0.5941
WEI	0.1473	0.2181	0.3266
VC	0.2279	0.3692	0.6385

Mezösi et al. [59] explored wind erosion sensitivity in Hungary using fuzzy logic memberships (0 to 1) for CF, soil erodibility (mt/ha/yr), and vegetative cover (NDVI) sensitivity to wind erosion. The authors applied the Lyles [49] formulation for CF (Eq. 4) based on average monthly wind velocity. A linear monotonically increasing membership for CF was assumed. Equal weights were given to the exponential monotonically increasing soil erodibility membership, the exponential monotonically decreasing vegetative cover membership, and the CF membership to prepare an area erosion sensitivity map.

The climatic factor (CF) is of particular importance with respect to weight in that it incorporates an index of wind intensity coupled with precipitation and temperature that consolidates key important attributes of wind erosion: threshold wind velocity and a surrogate for soil dryness. Figure 2 clearly demonstrates a common spring-like pattern for the CF across New Mexico, having a pronounced peak that trails off during summer and fall. Therefore, a location's sensitivity to wind erosion would be highest during the rising portion of the pattern, especially given potential increased soil erodibility due to multiple freeze-thaw cycles that frequently occur in New Mexico [61].

7.4. Wind Erosion Sensitivity (WES)

Based on the FAHP derived weights for CR, WEI, and VC, a wind erosion sensitivity for each location may be realized and be judged as high sensitivity, medium sensitivity, or low sensitivity Without verified field survey data of wind erosion soil loss, any threshold categorization is inherently arbitrary. The procedure, however, does suggest that Las Cruces is the most sensitive location for wind erosion with Los Alamos and Clines Corner as the least sensitive locations. High wind and blowing dust warnings are common occurrences in parts of southern New Mexico. Dust storm frequency worldwide is highest for desert/bare ground and shrubland regions, and comparatively low in grassland regions [62]. This region of the state has a predominance of desert and shrubland vegetative

land cover (USGS National Gap Analysis Program [63)] and, as such, is more susceptible to soil erosion by wind. Based on the results shown in column 5 of Table 4 and the methodology employed, a WES classification may be generalized as moderate to high sensitivity for weightings greater than 0.5; low to moderate sensitivity for a weighting between 0.2 and 0.5; and low sensitivity for weightings less than 0.2.

8. Conclusion

Prioritizing and assigning weights to key criteria is essential to effective decision making. Fuzzy Analytical Hierarchy Process (FAHP) is ideally suited for use in a Multi-Criteria Decision Making (MCDM) process, wherein human judgements in terms of linguistic phases obtained from multiple decision makers are represented as fuzzy numbers, enabling the final criteria weightings to account for the uncertainty and vagueness in use of linguistic variables by the decision makers. This uncertainty and vagueness in human judgement is captured and integrated using triangular fuzzy numbers (TFNs) and aggregated into a single pair-wise comparison matrix using the extent analysis method [54] to evaluate the weight of each criteria. The weights represent the degree of importance of a given criteria relative an overall criterion. For wind erosion sensitivity (WES), three criteria were identified and evaluated for thirteen landfill locations in New Mexico: climatic factor (CF) as a function of Wind Power Density (WPD) and Effective Precipitation Index, soil erodibility given as a wind erodibility index (WEI), and vegetation cover (VC) expressed as NDVI. CF is considered critical factor as it integrates the forcing function of threshold wind velocity obtained from the USDA WEPS model with a surrogate for soil dryness as related to average monthly precipitation and temperature. Specific locations within the state were generalized as having low, low to moderate, or moderate to high wind erosion sensitivity. Despite the uncertainties associated with data input, the technique provides for identification of potential hot spots for wind erosion with respect to the design and maintenance of final cover for landfills in New Mexico. Incorporating site-specific ground truth information to improve estimates of soil erodibility and vegetative cover will increase the validity of WES assessment.

References

[1] Yan, H., Wang, S., Wang, C., Zhang, G., and Patels, N. (2005). Losses of soil organic carbon under wind erosion in China, Global Change Biology, 11, 828-840.

[2] Li, J., Okin, G. S., Alvarez, L., and Epstein, H. (2007). Quantitative effects of vegetation cover on wind erosion and soil nutrient loss in a desert grassland of southern New Mexico, USA. Biogeochemistry, 85, 317-332.

[3] Hagen, L. J., Wagner, L. E., Tatarko, J., Skidmore, E. L., Durar, A. A., Steiner, J. L., Schomberg, H. H., Retta, A., Armbrust, D. V., Zobeck, T. M., Unger, P. W., Ding, D., Elminyawi, I. (1995). Wind Erosion Prediction System: technical description, In: Proceedings of WEPP/WEPS Symposium, August 9-11, Des Moines, IA, Soil and Water Conservation Society, Ankeny, IA.

[4] Asuquo, D. E. and Onuodu, F. E. (2016). A fuzzy AHP model for selection of university academic staff, International Journal of Computer Applications, 141 (1), 19-26.

[5] Forman, E. and Peniwati, K. (1998). Aggregating individual judgements and priorities with the analytic hierarchy process, European Journal of Operations Research, 108 (1), 165-169.

[6] Woodruff, N. P., and Siddoway, F. H. (1965). A wind erosion equation, Soil Science Society of America Proceedings, 29, 602-608.

[7] Anderson, C. H. and Wendhardt, A. (1966). Soil erodibility, fall and spring, Canadian Journal of Soil Science, 46, 255-259.

[8] Wang, L., Shi, Z. H., Wu, G. L., and Fang, N. F. (2014). Freeze/thaw and soil moisture effects on wind erosion, Geomorphology, 207, 141-148.

[9] Belnap, J. and Gillette, D. A. (1998). Vulnerability of desert biological soil crusts to wind erosion: the influence of crust development, soil texture, and disturbance, Journal of Arid Environments, 39, 133-142.

[10] Fryrear, D. W., Krammes, C. A., Williamson, D. L., and Zobeck, T. M. (1994). Computing the wind erodible fraction of soils, Journal of Soil and Water Conservation, 49 (2), 183-188.

[11] Zhou, Y., Guo, B., Wang, S. X., and Tao, H. P. (2015). An estimation method of soil wind erosion in Inner Mongolia of China based on geographic information system and remote sensing, Journal of Arid Land, 7 (3), 304-317.

[12] USDA Web Soil Survey, https://websoilsurvey.nrcs.usda.gov/.

[13] Mirmousavi, S. H. (2016). Regional modeling of wind erosion in north west and south west Iran, Eurasian Soil Science, 49 (8), 942-953.

[14] Chepil, W. S. (1956). Influence of moisture on erodibility of soil by wind, Soil Science Society of America Proceedings, 20, 288-292.

[15] Sirjani, E., Sameni, A., Moosai, A. A., Mahmoodabadi, M., Varoei, M. M., and Laurent, B. (2018). Assessment of wind erosion rate affected by different soil properties in the Fars province, Iran, International Conference on Aeolian Research, June 25-29, Bordeaux, France.

[16] Weinan, C., Zhibao, D., Zhenshan, L., and Zuotao, Y. (1996). Wind tunnel test of the influence of moisture on the erodibility of loessial sandy loam soils by wind, Journal of Arid Environments, 34, 391-402.

[17] Thornthwaite, C. W. (1931). The climates of North America according to a new classification. Geographical Review, 21 (4), 633-655.

[18] Gamo, M., Shinoda, M., and Maeda, T. (2013). Classifications of arid lands, including soil degradation and irrigated areas, based on vegetation and aridity indices, International Journal of Remote Sensing, 34 (19), 6701-6722.

[19] Ravi, S., Zobeck, T. M., Over, T. M., Okin, G. S., and D'Odorico, P. (2006). On the effect of moisture bonding forces in air-dry soils on threshold friction velocity of wind erosion, Sedimentology, 53, 597-609.

[20] Chepil, W. S. (1945). The transport capacity of the wind, Soil Science, 69, 475-480.

[21] Van Donk, S. J., Wagner, L. E., Skidmore, E. L., and Tatarko, J. (2005). Comparison of the Weibull model with measured wind speed distributions for stochastic wind generation, Transactions of the ASAE, 48 (2), 503-510.

[22] Painter, D. J. (1977). Wind erosion summaries for New Zealand sites, Project Report P/15, New Zealand Agricultural Engineering Institute, Lincoln College, Canterbury, New Zealand.

[23] Fry, J., Xian, G., Jin, S., Dewitz, J., Homer, C., Yang, L., Barnes, C., Herold, N., & Wickham, J. (2011). Completion of the 2006 National Land Cover Database for the Conterminous United States. Photogrammetric Engineering and Remote Sensing, *77*, 858−864.

[24] Raupach, M. R., Gillette, D. A., and Leys, J. F. (1993). The effect of roughness elements on wind erosion threshold, Journal of Geophysical Research, 98 (D2), 3023-3029.

[25] Munson, S. M., Belnap, J., and Okin, G. (2011). Responses of wind erosion to climate-induced vegetation changes on the Colorado Plateau, PNAS, 108 (10), 3854-3859.

[26] Meng, Z., Dang, X., Gao, Y., Ren, X., Ding, Y., and Wang, M. (2018). Interactive effects of wind speed, vegetation coverage, and soil moisture in controlling wind erosion in a temperature desert steppe, Inner Mongolia of China, Journal of Arid Land, 10 (4), 534-547.

[27] Yan, Y., Xin, X., Xu, X., Wang, X., Yang, G., Yan, R., and Chen, B. (2013). Quantitative effects of wind erosion on the soil texture and soil nutrients under different vegetation coverage in a semiarid steppe of northern China, Plant Soil, 369, 585-598.

[28] West, H., Quinn, N., Horswell, M., and White, P. (2018). Assessing vegetation response to soil moisture fluctuation under extreme drought using Sentinel-2, Water, 10 (7), 838, DOI: 10.3390/w10070838.

[29] Weltz, M. A., Arslan, A. B., and Lane, L. J. (1992). Hydraulic roughness coefficients for native rangelands, Journal of Irrigation and Drainage Engineering, 118 (5), 776-790.

[30] Anderson, C. E., and Stormont, J. C. (2005). Gravel admixtures for erosion protection in semi-arid climates, Erosion of Soils and Scour of Foundations, Proceedings of Geo-Frontiers 2005, January 24-26, Austin, Texas.

[31] Breshears, D. D., Nyhan, J. W., and Davenport, D. W. (2005). Ecohydrology monitoring and excavation of semiarid landfill covers a decade after installation, Vadose Zone Hydrology, 4, 788-910.

[32] Dwyer, S., McClellan, Y., Reavis, B., Dwyer, B., Newman, G. and Wolters, G. L. (2001). Analysis of vegetative on six different landfill cover profiles in an arid environment, Sandia National Laboratories, SAND2005-29492949.

[33] Weiss, J. L., Gutzler, D. S., Allred-Coonrod, J. E., and Dahm, C. N. (2004). Long-term vegetation monitoring in a diverse semi-arid setting, central New Mexico, USA, Journal of Arid Environments, 58, 249-272.

[34] Shi, H., Gao, Q., Qi, Y., Liu, J., and Hu, Y. (2010). Wind erosion hazard assessment of the Mongolian Plateau using FCM and GIS techniques, Environmental Earth Sciences, 61, 689-697.

[35] Ko, D. W., Kim, D., Narantsetseg, A., and Kang, S. (2017). Comparison of field- and satellite-based vegetation cover estimation methods, Journal of Ecology and Environment, 41 (5), DOI 10.1186/s41610-016-0022-z.

[36] Fern, R. R., Foxley, E. A., Bruno, A., and Morrison, M. L. (2018). Suitability of NDVI and OSAVI as estimators of green biomass and coverage in a semi-arid rangeland. Ecological Indicators, 94, 16-21.

[37] Saadoud, D., Hassani, M,. Peinado, F. J. M., and Guettouche, M. S. (2018). Application of fuzzy logic approach for wind erosion hazard mapping in Laghouat region (Algeria) using remote sensing and GIS, Aeolian Research, 32, 24-34.

[38] Bannari, A., Morin, D., Bonn, F., and Huete, A. R. (1995). A review of vegetation indices, Remote Sensing Reviews, 13, 95-120.

[39] Bulut, G. G., Cal, M. P., Richardson, C. P. and Gallegos, J. B. (2012). A GIS-Based Soil Erosion Risk Map for New Mexico. New Mexico Journal of Science, 46, 27-37.

[40] Hagen, S. C., Heilman, P., Marsett, R., Torbick, N., Salas, W., van Ravensway, J., and Qi, J. (2012). Mapping total vegetation cover across western rangelands with moderate-resolution imaging spectroradiometer data, Rangeland Ecology & Management, 65, 456-467.

[41] Cole, G. W., Lyles, L. and Hagen, L. J. (1983). A simulation model of daily wind erosion soil loss, Transactions of the ASAE Paper 82-2575, 1758-1765.

[42] Potter, K. N., Williams, J. R., Larney, F. J., and Bullock, M. S. (1998). Evaluation of EPIC's wind erosion submodel using data from southern Alberta, Canadian Journal of Soil Science, 78 (3), 485-492.

[43] Gurjar, G. N., Swami, S., Telkar, S. G., Meena, N. K., and Singh, S. (2017). Concepts of wind erosion and factors affecting the rate of soil loss through the action of wind, Biomolecule Reports-An International eNewsletter. BR/10/17/02.

[44] Schmidt, S. Meusburger, K., de Figueiredo, T., and Alewell, C. (2017). Modelling hot spots of soil loss by wind erosion (SoLoWind) in western Saxony, Germany, Land Degradation & Development, 28, 1100-1112.

[45] Fryrear, D. W. and Saleh, A. (1996). Wind erosion: field length, Soil Science, 161 (6), 398-404.

[46] Stout, J. E. (1990). Wind erosion within a simple field, Transactions of the ASAE, 33 (5), 1597-1600.

[47] Zhang, J., Yang, M., Deng, X., Liu, X., Zhang, F., and Zhou, W. (2018). Beryllium-7 measurements of wind erosion on sloping fields in the wind-water erosion crisscross region on the Chinese Loess Plateau, Science of the Total Environment, 615, 240-252.

[48] NM Climate Center, New Mexico State University, https://weather.nmsu.edu/.

[49] Ravi, S., D'Odorico, P., Over, T. M., and Zobeck, T. M. (2004). On the effect of air humidity on soil susceptibility to wind erosion: The case of air-dry soils. Geophysical Research Letters, 31, L09051.

[50] Lyles, L. (1983). Erosive wind energy distributions and climatic factors of the west, Journal of Soil and Water Conservation, 38 (2), 106-109.

[51] Chepil, W. S., Siddoway, F. H. and Armbrust, D. V. (1962). Climatic factor for estimating wind erodibility of farm fields, Journal Soil and Water Conservation, 17 (4), 162-165.

[52] US Climate Data, https://www.usclimatedata.com/.

[53] Saaty, T. L. (1980). The Analytic Hierarchy Process. McGraw-Hill, New York.

[54] Chang, D. Y. (1996). Applications of the extent analysis method on fuzzy AHP, European Journal of Operations Research, 95, 649-655.

[55] Wang, Y. M., Elhag, T. M. S., Hua, Z. S. (2006). A modified fuzzy logarithmic least squares method for fuzzy analytic hierarchy process. Fuzzy Sets and Systems, 157 (23), 3055-3071.

[56] Jie, L. H., Meng, M. C., and Cheong, C. W. (2006). Web based fuzzy multicriteria decision making tool, International Journal of the Computer, the Internet and Management, 14 (2), 1-14.

[57] USDA Natural Resources Conservation Service, Wind Erosion Prediction System https://www.nrcs.usda.gov/wps/portal/nrcs/main/national/technical/tools/weps/.

[58] Torno, S., Toraño, J., Menendez, M., Gent, M., and Allende, C. (2011). Prediction of particulate air pollution from a landfill site using CFD and LIDAR techniques, Environmental Fluid Mechanics, 11, 99-112.

[59] Mezösi, G., Blanka, V., Bata, T., Ladányl, Z., Kemény, G., and Meyer, B. C. (2016). Assessment of future scenarios for wind erosion sensitivity changes based on ALADIN and REMO regional climate model simulation data, Open Geosciences, 8, 465-477.

[60] Guo, B., Zhang, F. F., Yang, G., Sun, C. H., Han, F. and Jiang, L. (2017). Improved estimation method of soil wind erosion based on remote sensing and geographic information system in the Xinjiang Uygur Autonomous Region, China, Geomatics Natural Hazards and Risk, 8 (2), 1752-1767.

[61] Hershfield, D. M. (1974). The frequency of freeze-thaw cycles, Journal of Meteorology, 13, 348-354.

[62] Engelstaedter, S., Kohfeld, K. E., Tegen, I., and Harrison, S. P. (2003). Controls of dust emissions by vegetation and topographic depressions: an evaluation using dust storm frequency data, Geophysical Research Letters, 30 (6), 1294.

[63] USGS National Gap Analysis Program, https://gapanalysis.usgs.gov/.